

Environmental Science Processes & Impacts

Accepted Manuscript



This is an *Accepted Manuscript*, which has been through the Royal Society of Chemistry peer review process and has been accepted for publication.

Accepted Manuscripts are published online shortly after acceptance, before technical editing, formatting and proof reading. Using this free service, authors can make their results available to the community, in citable form, before we publish the edited article. We will replace this *Accepted Manuscript* with the edited and formatted *Advance Article* as soon as it is available.

You can find more information about *Accepted Manuscripts* in the [Information for Authors](#).

Please note that technical editing may introduce minor changes to the text and/or graphics, which may alter content. The journal's standard [Terms & Conditions](#) and the [Ethical guidelines](#) still apply. In no event shall the Royal Society of Chemistry be held responsible for any errors or omissions in this *Accepted Manuscript* or any consequences arising from the use of any information it contains.



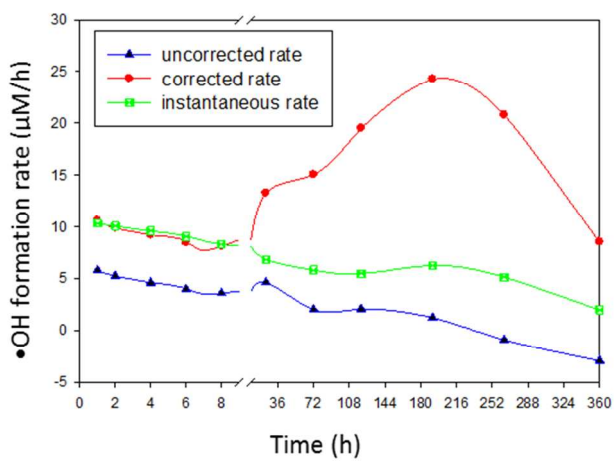
rsc.li/process-impacts

Environmental Impact Statement for:

Manuscript ID EM-ART-11-2013-000587

Title: Estimating OH radical photochemical formation rates in natural waters during long-term laboratory irradiation experiments (Sun et al.)

The hydroxyl ($\cdot\text{OH}$) radical is known to be generated by photochemical reactions in natural waters. As the most oxidative reactant among the active oxygen species, it plays an important role in the transformation and oxidation of a variety of organic and inorganic compounds, including priority pollutants. Thus, estimation of its formation rate is significant for understanding these processes; however, its accurate estimation during long-term laboratory irradiations (days to weeks) has been problematic. This paper examines different approaches for accurately determining $\cdot\text{OH}$ radical formation rates in natural waters using either short-term (hours) or long-term irradiations. It also discusses possible pathways of $\cdot\text{OH}$ formation in long-term irradiations in relation to hydrogen peroxide and iron concentrations. The merit of this study is not only methodological improvement, but it also provides better understanding of phototransformation pathways of dissolved organic matter (DOM).



“Uncorrected rate, corrected rate and instantaneous rate of $\bullet\text{OH}$ photoproduction in Dismal Swamp water.”

1 Estimating hydroxyl radical photochemical formation rates in natural 2 waters during long-term laboratory irradiation experiments

3 Luni Sun; Hongmei Chen; Hussain A. Abdulla; Kenneth Mopper*

5 **Abstract**

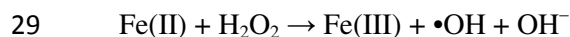
6 In this study it was observed that, during long-term irradiations (> 2 days) of natural waters, the
7 methods for measuring hydroxyl radical ($\bullet\text{OH}$) formation rates based upon sequentially determined
8 cumulative concentrations of photoproducts from probes significantly underestimate actual $\bullet\text{OH}$
9 formation rates. Performing a correction using the photodegradation rates of the probe products improves
10 the $\bullet\text{OH}$ estimation for short term irradiations (< 2 days), but not long term irradiations. Only the
11 'instantaneous' formation rates, which were obtained by adding probes at each time point and irradiating
12 the water sample (or sub-sample) for a short time (≤ 2 h), were found appropriate for accurately estimating
13 $\bullet\text{OH}$ photochemical formation rates during long-term laboratory irradiation experiments. Our results also
14 showed that in iron- and dissolved organic matter (DOM)-rich water samples, $\bullet\text{OH}$ appears to be mainly
15 produced from the Fenton reaction initially, but subsequently from other sources possibly from DOM
16 photoreactions. Pathways of $\bullet\text{OH}$ formation in long-term irradiations in relation to H_2O_2 and iron
17 concentrations are discussed.

19 **Introduction**

20 The hydroxyl radical ($\bullet\text{OH}$) is the most oxidative reactant among the reactive oxygen species, it plays
21 an important role in the transformation and oxidation of a variety of organic and inorganic compounds^{1,2}.
22 Photochemical reactions are the major sources of $\bullet\text{OH}$ radical in natural waters. The photo-formation of
23 $\bullet\text{OH}$ depends on its major sources in sunlit waters, which include DOM photoreactions, the photo-Fenton
24 reaction, and nitrate and nitrite photolyses³. Nitrate and nitrite photolyses are often found to be important
25 sources⁴, in rivers where their contributions are 1~89 % from nitrate and 2~70 % from nitrite, while in
26 seawaters their contributions are 7~75 % from nitrate and 1~8 % from nitrite³. However, in iron-rich
27 waters, the contribution of the photo-Fenton reaction (see below) can account for more than 70% the of
28 total photochemical $\bullet\text{OH}$ production⁵⁻⁷.

Department of Chemistry and Biochemistry, Old Dominion University, Norfolk, VA

* Corresponding author. Email: kmopper@odu.edu. Tel: 757-683-4094 Fax: 757-683-5310



30 where Fe(II) and Fe(III) include the hydrated and DOM-complexed iron species. In seawater and high
31 DOM freshwaters, DOM photoreactions appear to be the main source for $\bullet\text{OH}^{2,8-12}$. Reactions involving
32 hydroquinolic and phenolic moieties within humic substances appear to be responsible, at least in part, for
33 $\bullet\text{OH}$ photoproduction in these waters^{2, 8}.

34 In natural waters, photochemical formation rates of $\bullet\text{OH}$ are determined indirectly using probes. The
35 probe reactions can be split into two broad categories: 1) $\bullet\text{OH}$ addition to probes, with $\bullet\text{OH}$ either being
36 added to the carbon atoms in probes such as 4-nitrophenol, nitrobenzene, benzene, benzoic acid, and
37 terephthalate, or being added to the sulfoxide group in probes, e.g. dimethyl-sulfoxide; and 2) abstraction
38 of a hydrogen atom on the probes such as methanol, formic acid, methane and butyl chloride^{8, 13, 14}.

39 Among these probes, benzene and benzoic acid have been commonly used. Typically, the probes are
40 added initially to the samples and the cumulative concentrations of phenolic products are measured after
41 irradiating for several minutes¹⁵ or hours^{3, 10, 16, 17}. These phenolic product compounds are non- or very
42 weak absorbers of light in the solar irradiance spectrum and thus do not undergo direct photoreaction;
43 however, in natural waters, their phototransformation/destruction may be promoted by the presence of
44 DOM, possibly through electron or hydrogen atom transfer from reactive excited triplet states of DOM¹⁸,
45 ¹⁹, or reaction with reactive oxygen species, such as hydrogen peroxide²⁰, and singlet oxygen²¹. Thus,
46 during long-term irradiations, this loss may lead to significant underestimation of the cumulative
47 concentrations of phenolic products. This underestimation is likely minor when only initial $\bullet\text{OH}$
48 formation rates are taken into account¹⁷, but it may be significant for time-course studies of $\bullet\text{OH}$
49 formation rates or its steady-state concentration, such as studies on the sources of $\bullet\text{OH}$ which usually
50 require several hours to adequately measure the generation of $\bullet\text{OH}^{3, 6, 16}$. For example, in studies
51 examining the photo-Fenton reaction in natural waters, the $\bullet\text{OH}$ formation rate, and H_2O_2 and Fe (II)
52 concentrations were measured hourly under different experimental conditions⁷. Moreover, DOM
53 photochemical transformation studies usually run for hours to days²²⁻²⁴. Since DOM is an important
54 source and sink of $\bullet\text{OH}$ (as well as other reactive species), accurate estimation of $\bullet\text{OH}$ can improve our
55 understanding of DOM transformation pathways. Therefore, it is necessary to establish the stability of
56 both the $\bullet\text{OH}$ probe compound and the quantified product species with respect to direct and indirect
57 photolysis in natural waters²⁵.

58 In this study, we estimated time-course $\bullet\text{OH}$ formation rates in DOM-rich water (Great Dismal
59 Swamp) and estuarine water by two approaches: 1) correcting for product loss and 2) obtaining near-
60 instantaneous formation rates. The corrected formation rates were obtained by adding the
61 photodegradation rates of corresponding products to their formation rates, and the instantaneous rates

62 were obtained by adding probes at each time point and irradiating the sample for a short time (≤ 2 h).
63 Moreover, we discuss possible pathways of $\bullet\text{OH}$ formation in iron- and DOM-rich samples during long-
64 term irradiations.

65

66 **Experimental**

67 **Chemicals**

68 Phenol (purity grade $>99\%$), sodium benzoate (99.5%), benzene (HPLC grade), and desferrioxamine
69 mesylate (DFOM) (92.5%) were obtained from Sigma; salicylic acid (SA) (99%) was obtained from
70 Fisher; H_2O_2 (35% w/w) and methanol (HPLC grade) were obtained from Acros. Ultra-pure water (Milli-
71 Q water, $>18\text{ M}\Omega\text{cm}^{-1}$) was used for solution preparation.

72

73 **Sample description**

74 Water samples were freshly obtained from the Great Dismal Swamp (near 36.7°S and 76.4°W , salinity
75 0 ppm , $\text{pH } 3.7$) and Elizabeth River estuary (near 36.9°S and 76.3°W , salinity 20 ppm , $\text{pH } 7.5$) in spring
76 2013. Samples were filtered within 24 hours of collection through a pre-cleaned $0.1\ \mu\text{m}$ capsule filter
77 (Polycap TC, Whatman). Dissolved organic carbon (DOC) and total dissolved nitrogen (TDN) were 54
78 ppm and 1.9 ppm for the Great Dismal Swamp sample, and 3 ppm and 0.9 ppm for the Elizabeth River
79 estuarine sample.

80

81 **Irradiations**

82 All samples were placed into quartz tubes or flasks and kept oxygenated by periodic shaking in air.
83 Irradiations were conducted using a solar simulator containing UVA340 bulbs (Q-Panel). The solar
84 simulator is described elsewhere²⁶. These lamps have a spectral output nearly identical to natural sunlight
85 from ~ 295 to $\sim 360\text{ nm}$ (<http://www.solarsys.biz/0103.shtml>). In a comparison of the light output from the
86 solar simulator to natural sunlight, the solar simulator provided 127% of the photobleaching occurring
87 under winter mid-day sunlight at 36.89°N latitude²⁷. Consequently, the $\bullet\text{OH}$ production rates in this study
88 are likely somewhat higher than in the environment. Dark controls were wrapped in foil and placed inside
89 the solar simulator. All samples were irradiated at room temperature and at their natural concentrations
90 and pH in order to approximately simulate surface conditions, and to avoid potential contamination.

91

92 **Determination of $\bullet\text{OH}$ formation rate**

93 Probe compounds (sodium benzoate or benzene) were added to aliquots of the water sample to final
94 concentrations of 5.0 mM and 3.0 mM respectively. Complete dissolution of benzene was facilitated by

95 vigorous stirring at room temperature. These samples were used to determine the effect of long-term,
96 continuous irradiation of the •OH probes. Other aliquots of the water sample were used for measuring
97 instantaneous •OH formation rates and parameters including DOC, TDN, DFe and H₂O₂ production. The
98 instantaneous •OH formation rates were determined by irradiating the latter aliquots without the probes
99 present; subsamples were then removed at specific time points and irradiated for ≤2h with the •OH
100 probes.

101 Benzoic acid reacts with •OH to form SA and other products, while benzene reacts to form phenol and
102 other products. The fraction of SA (or phenol) formed relative to the other •OH photoproducts is
103 constant¹⁰ thereby enabling the use of SA (or phenol) production to determine the total •OH production,
104 as described below. The SA and phenol photoproducts were measured using HPLC with fluorescence
105 detection as described in detail elsewhere^{10, 29}; the excitation/emission wavelengths were 300/400 nm⁹ for
106 SA and 260/310 nm for phenol²⁸, respectively. Cumulative SA and/or phenol concentrations were plotted
107 vs. irradiation time. The observed photo-formation rates of SA and phenol (R_{ob}) were determined from the
108 tangent slopes at each time point of the curve using Matlab. R_{ob} was used to evaluate the uncorrected •OH
109 photo-production rate, R_{unc}, which was calculated by the following equation:

$$110 \quad R_{\text{unc}} = \frac{R_{\text{ob}} \times F}{Y} \quad (1)$$

111 where Y is the yield of photoproduct formed per probe molecule oxidized by •OH. Since the reaction
112 between probe and •OH forms more than one product^{10, 29}, this value is always less than 100 % (see
113 Results and Discussion). F is a calibration factor, which is related to the fraction of the •OH flux that
114 reacts with the probe and accounts for competing OH scavengers in natural waters, such as DOM. F is
115 evaluated for each sample type by competition kinetics using a series of different probes concentrations as
116 described in detail by Zhou and Mopper³⁰. For our experiments, F was 1.11~1.26, depending on the
117 probes and sample types.

118

119 **Determination of photodegradation rates of •OH probe products**

120 Photodegradation rates of SA and phenol were obtained by irradiating 40 μM SA and 180 μM phenol
121 in the Dismal Swamp sample and measuring their concentrations over 24 h. The concentrations of SA
122 and phenol chosen were close to the maximum cumulative concentrations formed in our irradiation
123 experiments.

124

125 **Determination of dissolved organic carbon (DOC)/total dissolved nitrogen (TDN), dissolved iron** 126 **(DFe) and H₂O₂ production**

127 DOC and TDN were measured for all samples using high temperature (720°C) catalytic combustion on
 128 a Shimadzu TOC-V-CPH carbon analyzer. DFe concentration and H₂O₂ production were measured for
 129 Dismal Swamp sample. DFe was measured using a Hitachi Z8100 polarized Zeeman flame atomic
 130 absorption spectrophotometer equipped with an iron hollow cathode lamp; and H₂O₂ production was
 131 measured by modified (p-hydroxyphenyl)-acetic acid dimerization method³¹.

132

133 Results and Discussions

134 Calibration of Y_{ph} value

135 Y is the yield of photoproduct formed per probe molecule oxidized by •OH. Most Y values of SA (Y_{SA})
 136 from published radiolysis experiments are 17~18%^{10, 14, 32} while the values of phenol (Y_{ph}) range from
 137 66% to 95%^{14, 33-35}; the high Y_{ph} of 95% was observed during nitrate photolysis³⁵. Because of the wide
 138 range of published Y_{ph} values, we did not select a Y_{ph} value for our system from published data. Instead,
 139 we used the much less variable Y_{SA} value (17%¹⁰) to calibrate the Y_{ph} value by using H₂O₂ photolysis as a
 140 pure •OH source. Different concentrations of H₂O₂ were added to solutions containing sodium benzoate
 141 or benzene and irradiated for 1 h. Assuming the degradation of SA and phenol is negligible in this short
 142 period, at the same concentrations of H₂O₂, the •OH photoproduction rate R_{unc} should be the same for
 143 both probes, that is:

$$144 \quad R_{\text{unc}} = \frac{R_{\text{SA}} \times F_{\text{SA}}}{Y_{\text{SA}}} = \frac{R_{\text{ph}} \times F_{\text{ph}}}{Y_{\text{ph}}} \quad (2)$$

145 but, since there are no other competing scavengers, F_{SA}=F_{ph}=1:

$$146 \quad R_{\text{unc}} = \frac{R_{\text{SA}}}{Y_{\text{SA}}} = \frac{R_{\text{ph}}}{Y_{\text{ph}}} \quad (3)$$

147 Y_{ph} was then calculated as:

$$148 \quad Y_{\text{ph}} = \frac{Y_{\text{SA}} \times R_{\text{ph}}}{R_{\text{SA}}} \quad (4)$$

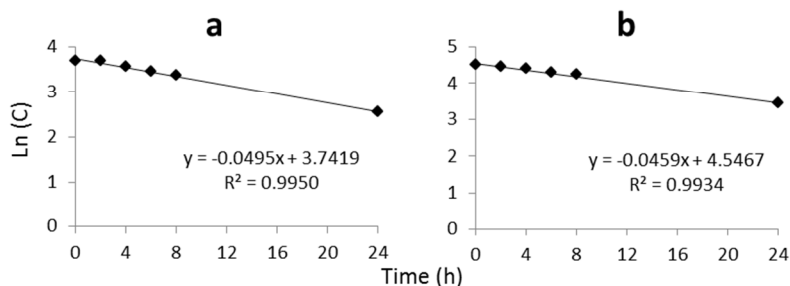
149 In our experiments, Y_{ph} value was calculated as 69.3±2.2 %, which was then used for all calculations.

150 This value is in agreement with most published values²¹⁻²⁴.

151

152 Corrections of •OH formation rates

153 Photodegradation was observed for both SA and phenol, and followed first order reaction kinetics. The
 154 photodegradation rate at each time point is $k[\text{SA or phenol}]_t$, where k is the slope of the plot of Ln
 155 (concentration) vs. the irradiation time; it is -0.0495 h⁻¹ for SA and -0.0459 h⁻¹ for phenol (Fig. 1).



156
 157 Fig. 1 SA (a) and phenol (b) photodegradation in the Dismal Swamp sample over a 24 h irradiation in a UV solar
 158 simulator. Subsamples for measuring SA and phenol degradation rates were taken at the same time as the \bullet OH
 159 measurements.

160
 161 The corrected photoformation rate of SA or phenol is the observed SA (or phenol) formation rate (R_{ob})
 162 plus its degradation rate. Therefore, the \bullet OH formation rate (R_{cor}) was corrected and calculated by the
 163 following equation:

$$164 \quad R_{cor} = \frac{R_{ins} - R_{unc}}{1 - R_{unc}/R_{ins}} = R_{unc} + \frac{R_{ins} R_{unc}}{1 - R_{unc}/R_{ins}} \quad (5)$$

165 Uncorrected \bullet OH formation rate (R_{unc}), corrected formation rate (R_{cor}), and instantaneous formation
 166 rates (R_{ins}) at each time point during 15 d are shown in Fig. 2 and Fig. 3. R_{ins} was assumed to be the true
 167 \bullet OH formation rate; i.e., the degradation of SA or phenol is negligible for a one hour irradiation (Fig. 1).
 168 The negative R_{unc} values at the longer irradiation times (Fig. 2 and Fig. 3) is probably due to the
 169 substantial photodegradation of the probe photoproducts upon long-term irradiation.

170 Comparison of \bullet OH formation rates

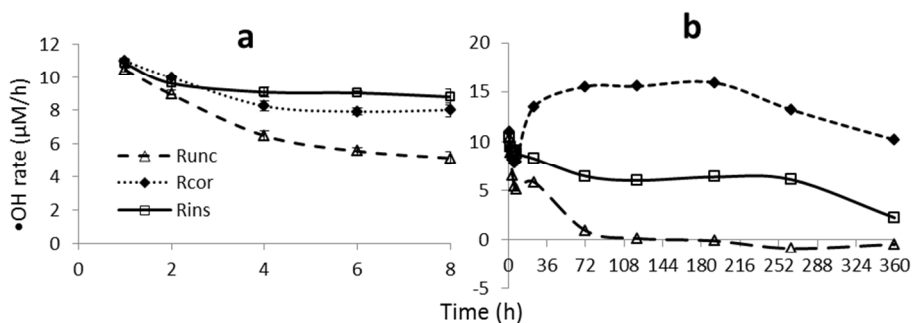
171 Between 2h and 8 h, R_{unc} values were lower than R_{ins} values (Table 1). The differences averaged 29 %
 172 using benzoic acid and 16% using benzene as probes; thus R_{OH} significantly underestimated \bullet OH
 173 formation. By performing corrections for probe product degradation, the agreement improved. The
 174 differences between R_{cor} and R_{ins} averaged 8 % using benzoic acid and 4% using benzene as probes.
 175 However, for longer irradiation periods (more than 8 h), neither R_{unc} nor R_{cor} agreed well with R_{ins} , as
 176 differences were >30 %. The reason for the large discrepancies might be that the added probes changed
 177 DOM photodegradation and OH production pathways, which only became significant after long-term
 178 irradiations containing the probe. Therefore, for long-term irradiations (*e.g.*, > ~1 day) R_{ins} should be used
 179 to determine the OH production rate. There were no significant differences in R_{ins} between two different
 180 probes (paired t test, $P=0.1066$) for up to 15 days of irradiation (Fig. 4).

181

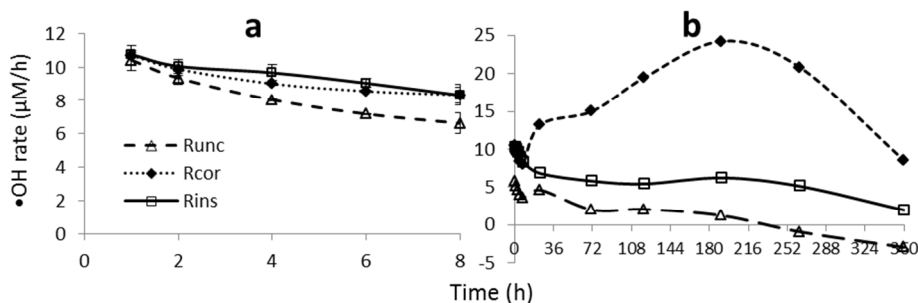
182 Table 1. Uncorrected $\bullet\text{OH}$ formation rate (R_{unc}), corrected formation rate (R_{cor}), and instantaneous formation rates
 183 (R_{ins}) during 8 h (n=2)

Time (h)	$\bullet\text{OH}$ formation rates ($\mu\text{M}/\text{h}$) by using					
	Benzoic acid			Benzene		
	R_{unc}	R_{cor}	R_{ins}	R_{unc}	R_{cor}	R_{ins}
1	10.5 ± 0.1	11.0 ± 0.1	10.8 ± 0.1	10.3 ± 0.5	10.6 ± 0.5	10.7 ± 0.1
2	9.0 ± 0.1	9.9 ± 0.1	10.1 ± 0.4	9.3 ± 0.4	9.9 ± 0.5	10.0 ± 0.4
4	6.5 ± 0.3	8.3 ± 0.3	9.6 ± 0.4	8.0 ± 0.1	9.0 ± 0.1	9.6 ± 0.5
6	5.6 ± 0.2	7.8 ± 0.2	9.0 ± 0.3	7.2 ± 0.1	8.6 ± 0.1	9.0 ± 0.3
8	5.2 ± 0.4	8.0 ± 0.4	8.3 ± 0.5	6.6 ± 0.6	8.1 ± 0.6	8.3 ± 0.5

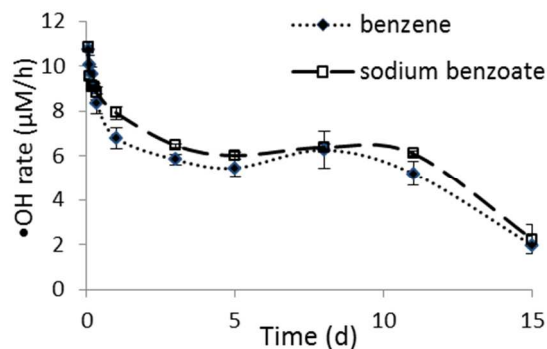
184



185
 186 Fig. 2 R_{unc} , R_{cor} and R_{ins} using benzoic acid as probe for 8 h (a) and 15 day (b) irradiations of Dismal Swamp water.
 187 Error bars are within the data points unless otherwise indicated.

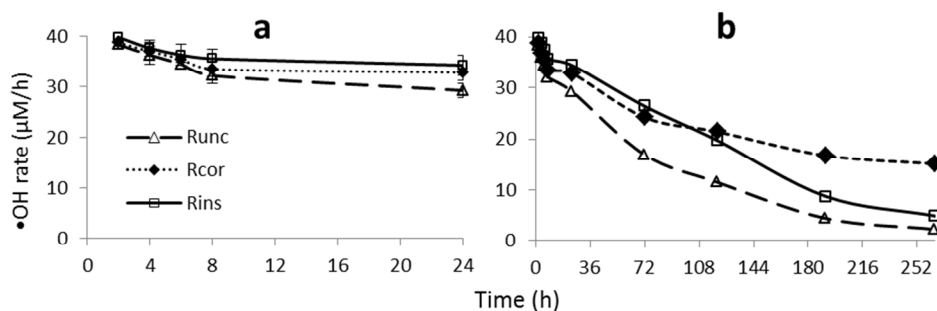


188
 189 Fig. 3. R_{unc} , R_{cor} and R_{ins} using benzene as probe for 8 h (a) and 15 day (b) irradiations of Dismal Swamp water.
 190 Error bars are within the data points unless otherwise indicated.



191
 192 Fig.4. Comparison of R_{ins} between two probes for a 15 day irradiation of Dismal Swamp water. Error bars are within
 193 the data points unless otherwise indicated.
 194

195 Measurements were also conducted in a low DOC (3 ppm) sample from the Elizabeth River (salinity of
 196 20). Only benzene was used as the $\bullet\text{OH}$ probe because it has higher Y and, thus a somewhat better
 197 selectivity than benzoic acid³⁶; and its corresponding photoproduct phenol has higher fluorescent intensity
 198 than SA. The photodegradation rate of phenol in the Elizabeth River sample was 0.00443 h^{-1} , which is
 199 only 1/10 of that for the Dismal Swamp water sample. $\bullet\text{OH}$ formation rates were also low in the Elizabeth
 200 River sample ($< 40 \text{ nM/h}$). However, this is not only due to low DOM, but also due to competing natural
 201 $\bullet\text{OH}$ scavengers including CO_3^{2-} and Br^- in saline water^{12, 37}. The t test showed no significant differences
 202 between R_{unc} , R_{cor} and R_{ins} during 6 h of irradiation ($P > 0.17$) (Fig. 5. a): thus, use of a correction or
 203 instantaneous rate was not necessary. However, significant differences were observed for irradiations $>$
 204 $\sim 24\text{h}$ (Fig. 5. b); thus the measurement of R_{ins} also appears to be necessary for long-term irradiations,
 205 even for this relatively low DOC sample.



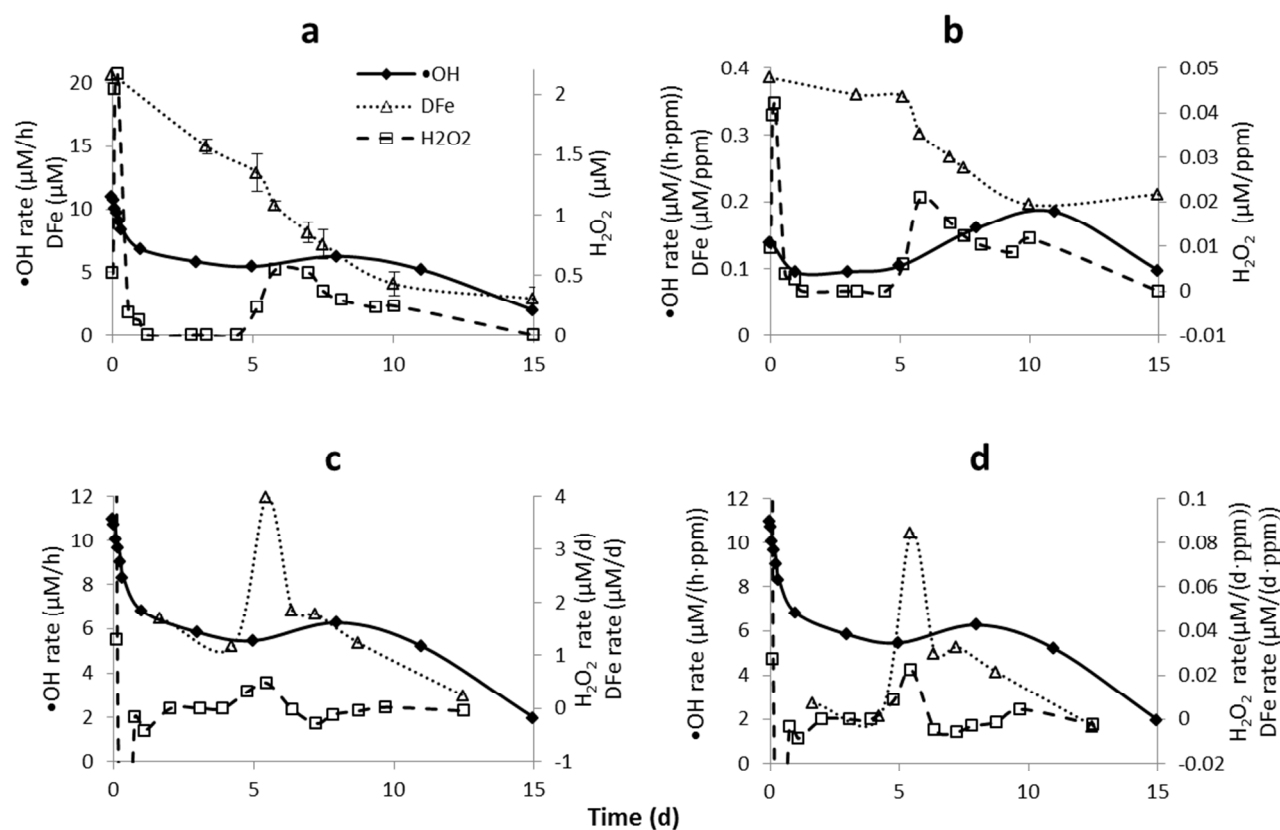
206
 207 Fig. 5. R_{unc} , R_{cor} and R_{ins} for 24 h and 11 day irradiations of Elizabeth River water. Error bars are within the data
 208 points unless otherwise indicated.
 209

210 **Possible $\bullet\text{OH}$ formation pathways in Dismal Swamp water**

211 R_{ins} values were positive through 15 days of continuous irradiation, and ranged from $\sim 10.5 \mu\text{M/h}$ on
212 day 1 to $\sim 2 \mu\text{M/h}$ on day 15 (Fig. 4). After day 1, the rate decreased until a plateau at $\sim 6 \mu\text{M/h}$ was
213 reached (from \sim day 3 to day 12), after which it dropped to $\sim 2 \mu\text{M/h}$ on day 15. During the irradiation,
214 DFe decreased from nearly $20 \mu\text{M}$ to $3 \mu\text{M}$ (Fig. 6a), and photochemically-induced flocculation was
215 observed after day 4. The photoproduction of H_2O_2 varied widely over the irradiation (Fig. 6c,d). H_2O_2
216 showed strong initial production, but fell to zero between day 2 and day 4, and then was produced again
217 after day 4 upon the onset of flocculation. We hypothesize that the photo-Fenton reaction was the main
218 source of the $\bullet\text{OH}$ initially, on the basis of high DFe and high H_2O_2 photoproduction from DOM during
219 the first day. Nitrate photolysis was likely a negligible source of $\bullet\text{OH}$ as the maximum $\bullet\text{OH}$ production
220 from nitrate was only $\sim 2.1 \times 10^{-3} \mu\text{M/h}$, based on a dissolved nitrogen concentration and assuming all
221 dissolved nitrogen was nitrate and assuming an $\bullet\text{OH}$ photo-production rate from nitrate of $\sim 1.1 \times 10^{-3} \mu\text{M}$
222 $\bullet\text{OH/h per } \mu\text{M nitrate}^{12, 37}$. To test for the effect of iron (i.e., the photo-Fenton reaction), an aliquot of
223 Dismal Swamp sample was irradiated with $100 \mu\text{M DFOM}$, which effectively binds all DFe into a
224 photochemically unreactive complex⁶. The DFOM addition reduced the $\bullet\text{OH}$ formation rate by about 90%
225 during an 8 h irradiation, thus confirming the initial importance of Fenton chemistry in $\bullet\text{OH}$
226 photoproduction in the Dismal Swamp sample. Between day 4 to day 7, H_2O_2 was again being
227 photoproduced (Fig. 6c, d), but a sharp decrease in DFe was also observed during this period, which is
228 likely decreased the importance of Fenton chemistry relative to OH photoproduction from other sources,
229 in particular DOM photoreactions²³. The reasons for the reappearance of H_2O_2 after day 4 are not known,
230 but may be related to major photochemically-induced changes in DOM composition and structure³⁸ and to
231 the initialization of DOM photoflocculation after day 4^{23, 39}. This is supported by the inverse relation
232 ($R^2=0.97$) between the DOC-normalized OH production rate and the DOC-normalized DFe concentration,
233 particularly after day 4 (Fig. 6b). To our knowledge, this behavior of H_2O_2 photoproduction has not been
234 previously observed and, thus, warrants further study. After day 10, as most DOM had been degraded or
235 mineralized, $\bullet\text{OH}$ formation decreased again.

236 It needs to be pointed out that, in addition to trapping the free $\bullet\text{OH}$, these probes (as well as most other
237 commonly used $\bullet\text{OH}$ probes) also react with other highly reactive hydroxylating species^{8, 40-42}: e.g.,
238 excited quinones triplets photochemically produce a species capable of hydroxylation, even though these
239 species exhibit reactivities about one an order of magnitude lower than the free $\bullet\text{OH}$ ⁴⁰. As quinone
240 structures were observed in the Dismal Swamp DOM by FTIR (unpublished data), it is likely that these
241 hydroxylating species contributed to the formation of hydroxylated compounds from the added probes.
242 Moreover, during the photo-Fenton reaction, the highly reactive and oxidizing ferryl ion, Fe(IV) , can be
243 formed, although at relatively low rates^{34, 43}. This species is capable not only of abstraction of a hydrogen

244 atom, even from methane⁴⁴, but also of aromatic and benzylic hydroxylation, *e.g.* conversion of benzene
 245 to phenol^{45, 46}. Although the ferryl ion is less oxidizing than the hydroxyl radical⁴⁷, we cannot reject its
 246 possible minor contribution to probe product formation in our iron rich system. Thus, in this study, all
 247 reported $\bullet\text{OH}$ production rates include both free $\bullet\text{OH}$ and any highly reactive species capable of
 248 hydroxylation the probe molecules. However, even if part of the probe product signal is due these other
 249 reactive species, they (in addition to $\bullet\text{OH}$) may have played role in the transformation of DOM, as DOC
 250 decreased about 75 % after 15 days irradiation, in agreement with Helms et al.³⁹. Details of
 251 phototransformation pathways of DOM will be further discussed in a future study.



252 Fig.6. (a) $\bullet\text{OH}$ formation rate, DFe and H_2O_2 concentration; (b) $\bullet\text{OH}$ formation rate, DFe and H_2O_2 concentration
 253 normalized to DOC; (c) $\bullet\text{OH}$ formation rate, DFe loss rate and H_2O_2 formation rate; (d) $\bullet\text{OH}$ formation rate, DFe
 254 loss rate, and H_2O_2 formation rate normalized to DOC during irradiation. $\bullet\text{OH}$ (\blacklozenge), H_2O_2 (\square), and DFe (\blacktriangle).
 255 Equivalent time points for iron and H_2O_2 were calibrated based on measured DOC in photodegraded subsamples
 256 relative to the original sample (DOC as %).
 257

258

259 Conclusions

260 In both DOM-rich and poor natural waters examined in this study, the methods for measuring •OH
261 formation rates by obtaining sequential cumulative concentrations of photoproducts from probes
262 substantially underestimated the actual •OH formation rate during long-term irradiations. Therefore, it is
263 recommended that instantaneous formation rates be used to estimate •OH photochemical formation rates
264 during long-term irradiation experiments, regardless of the probe used. For short-term irradiations of
265 natural waters, it is recommended that photodegradation rates of corresponding probe photoproducts be
266 determined in order to correct the OH production rate. Our results also showed that, in the iron- and
267 DOM-rich sample, •OH is likely produced mainly from the Fenton and photo-Fenton reactions initially,
268 but after that, •OH appears to be produced mainly by other pathways, in particular DOM photoreactions,
269 the mechanisms of which need to be further studied.

270

271 Acknowledgments

272 This research was supported by NSF grant OCE0850635 (to KM) awarded through the Chemical
273 Oceanography Program.

274

275 References

- 276 1. G. V. Buxton, C. L. Greenstock, W. P. Helman and A. B. Ross, *Phys. Chem. Ref. Data*, 1988, **17**,
277 513-886.
- 278 2. P. P. Vaughan and N. V. Blough, *Environmental Science & Technology*, 1998, **32**, 2947-2953.
- 279 3. K. G. Mostofa, C.-q. Liu, H. Sakugawa, D. Vione, D. Minakata, M. Saquib and M. A. Mottaleb, in
280 *Photobiogeochemistry of Organic Matter*, eds. K. M. G. Mostofa, T. Yoshioka, A. Mottaleb and D.
281 Vione, Springer Berlin Heidelberg, Editon edn., 2013, pp. 209-272.
- 282 4. J. Hoigné, C. Faust Bruce, R. Haag Werner, E. Scully Frank and G. Zepp Richard, in *Aquatic Humic*
283 *Substances*, American Chemical Society, Editon edn., 1988, vol. 219, pp. 363-381.
- 284 5. B. A. Southworth and B. M. Voelker, *Environmental Science & Technology*, 2003, **37**, 1130-1136.
- 285 6. E. White, P. Vaughan and R. Zepp, *Aquatic Sciences*, 2003, **65**, 402-414.
- 286 7. E. M. White, Ohio State University, 2000.
- 287 8. S. E. Page, W. A. Arnold and K. McNeill, *Environmental Science & Technology*, 2011, **45**, 2818-
288 2825.
- 289 9. J. Qian, K. Mopper and D. J. Kieber, *Deep Sea Research Part I: Oceanographic Research Papers*,
290 2001, **48**, 741-759.
- 291 10. X. Zhou and K. Mopper, *Marine Chemistry*, 1990, **30**, 71-88.
- 292 11. J. Qian, Washington State University, 1996.
- 293 12. K. Mopper and X. Zhou, *Science*, 1990, **250**, 661-664.
- 294 13. S. E. Page, W. A. Arnold and K. McNeill, *Journal of Environmental Monitoring*, 2010, **12**, 1658-
295 1665.
- 296 14. C. Anastasio and K. G. McGregor, *Atmospheric Environment*, 2001, **35**, 1079-1089.

- 297 15. T. Arakaki and B. C. Faust, *Journal of Geophysical Research: Atmospheres (1984–2012)*, 1998,
298 **103**, 3487-3504.
- 299 16. N. Nakatani, M. Ueda, H. Shindo, K. Takeda and H. Sakugawa, *Analytical Sciences*, 2007, **23**,
300 1137-1142.
- 301 17. F. al Housari, D. Vione, S. Chiron and S. Barbati, *Photochemical & Photobiological Sciences*, 2010,
302 **9**, 78-86.
- 303 18. S. Canonica, U. Jans, K. Stemmler and J. Hoigne, *Environmental science & technology*, 1995, **29**,
304 1822-1831.
- 305 19. K. S. Golanoski, S. Fang, R. Del Vecchio and N. V. Blough, *Environmental Science & Technology*,
306 2012, **46**, 3912-3920.
- 307 20. J. Beltran-Heredia, J. Torregrosa, J. R. Dominguez and J. A. Peres, *Chemosphere*, 2001, **42**, 351-
308 359.
- 309 21. F. Wilkinson, W. P. Helman and A. B. Ross, *Journal of Physical and Chemical Reference Data*,
310 1995, **24**, 663.
- 311 22. M. A. Moran and R. G. Zepp, *Limnology and Oceanography*, 1997, **42**, 1307-1316.
- 312 23. J. R. Helms, J. Mao, K. Schmidt-Rohr, H. Abdulla and K. Mopper, *Geochimica et Cosmochimica*
313 *Acta*, 2013, **121**, 398-413.
- 314 24. K. Mopper and D. J. Kieber, *The effects of UV radiation in the marine environment*, 2000, **10**,
315 101-129.
- 316 25. J. Burns, W. Cooper, J. Ferry, D. W. King, B. DiMento, K. McNeill, C. Miller, W. Miller, B. Peake, S.
317 Rusak, A. Rose and T. D. Waite, *Aquat. Sci.*, 2012, **74**, 683-734.
- 318 26. E. Minor, B. Dalzell, A. Stubbins and K. Mopper, *Aquat. Sci.*, 2007, **69**, 440-455.
- 319 27. J. R. Helms, A. Stubbins, J. D. Ritchie, E. C. Minor, D. J. Kieber and K. Mopper, *Limnology and*
320 *Oceanography*, 2008, **53**, 955.
- 321 28. K. Takeda, H. Takedoi, S. Yamaji, K. Ohta and H. Sakugawa, *Analytical sciences*, 2004, **20**, 153-
322 158.
- 323 29. S. P. Mezyk, T. J. Neubauer, W. J. Cooper and J. R. Peller, *The Journal of Physical Chemistry A*,
324 2007, **111**, 9019-9024.
- 325 30. K. Mopper, X. Zhou, R. J. Kieber, D. J. Kieber, R. J. Sikorski and R. D. Jones, *Nature*, 1991, **353**, 60-
326 62.
- 327 31. W. L. Miller and D. R. Kester, *Analytical Chemistry*, 1988, **60**, 2711-2715.
- 328 32. R. Matthews and D. Sangster, *The Journal of Physical Chemistry*, 1965, **69**, 1938-1946.
- 329 33. I. Loeff and G. Stein, *Journal of the Chemical Society (Resumed)*, 1963, 2623-2633.
- 330 34. I. Balakrishnan and M. P. Reddy, *The Journal of Physical Chemistry*, 1970, **74**, 850-855.
- 331 35. C. Minero, S. Chiron, G. Falletti, V. Maurino, E. Pelizzetti, R. Ajassa, M. Carlotti and D. Vione,
332 *Aquat. Sci.*, 2007, **69**, 71-85.
- 333 36. D. Vione, M. Ponzio, D. Bagnus, V. Maurino, C. Minero and M. Carlotti, *Environ Chem Lett*, 2010,
334 **8**, 95-100.
- 335 37. R. G. Zepp, J. Hoigne and H. Bader, *Environmental Science & Technology*, 1987, **21**, 443-450.
- 336 38. M. Gonsior, B. M. Peake, W. T. Cooper, D. Podgorski, J. D'Andrilli and W. J. Cooper,
337 *Environmental science & technology*, 2009, **43**, 698-703.
- 338 39. J. R. Helms, A. Stubbins, E. M. Perdue, N. W. Green, H. Chen and K. Mopper, *Marine Chemistry*,
339 2013, **155**, 81-91.
- 340 40. A. Pochon, P. P. Vaughan, D. Gan, P. Vath, N. V. Blough and D. E. Falvey, *The Journal of Physical*
341 *Chemistry A*, 2002, **106**, 2889-2894.
- 342 41. V. Maurino, D. Borghesi, D. Vione and C. Minero, *Photochemical & Photobiological Sciences*,
343 2008, **7**, 321-327.

- 344 42. W. J. Cooper, R. G. Zika, R. G. Petasne and A. M. Fischer, *Adv. Chem. Ser.*, 1989, **219**, 333-362.
- 345 43. S. H. Bossmann, E. Oliveros, S. Göb, S. Siegwart, E. P. Dahlen, L. Payawan, M. Straub, M. Wörner
346 and A. M. Braun, *The Journal of Physical Chemistry A*, 1998, **102**, 5542-5550.
- 347 44. K. Yoshizawa, Y. Shiota and T. Yamabe, *Journal of the American Chemical Society*, 1998, **120**,
348 564-572.
- 349 45. A. Bassan, M. R. A. Blomberg and P. E. M. Siegbahn, *Chemistry – A European Journal*, 2003, **9**,
350 4055-4067.
- 351 46. J. Baxendale and J. Magee, *Discussions of the Faraday Society*, 1953, **14**, 160-169.
- 352 47. W. Koppenol and J. F. Liebman, *The Journal of Physical Chemistry*, 1984, **88**, 99-101.

353